Available online at www.sciencedirect.com
SCIENCE DIRECT®
Journal of Sound and Vibration 265 (2003) 221–230
JOURNAL OF SOUND AND VIBRATION
www.elsevier.com/locate/jsvi

Letter to the Editor

A numerical study on the effects of design parameters on the performance and noise of a centrifugal fan

Wan-Ho Jeon*

Digital Appliance Research Lab., LG Electronics, 327-23, Kasan-dong, Kumchon-gu, Seoul 153-802, South Korea

Received 24 July 2002; accepted 27 November 2002

1. Introduction

The noise of blower and fan mainly consists of vibration-induced noise and flow-induced noise. In this paper, only the flow-induced noise is under consideration. The flow-induced noise is a branch of "Aeroacoustics", which is concerned with sound generated by aerodynamic forces or motions. Thus, in order to predict the source of the flow-induced noise and its characteristics, detailed information of the flow field has to be known priorly. However, the prediction of the flow-induced noise still remains a difficult area because the unsteady flow field of the centrifugal fan is hard to calculate. The numerical method to analyze the noise of a centrifugal fan has been developed by Jeon and Lee [1–3] This method can predict the acoustic pressure with an accuracy of maximum 2 dB error, compared with the measured data. The impeller is assumed to rotate with a constant angular velocity. The flow field in the impeller is considered as incompressible and inviscid. Based on these assumptions, the discrete vortex method (DVM) is used to describe the flow field in the centrifugal fan. The force acting on each element of the blade is calculated by the unsteady Bernoulli equation. In order to obtain acoustic farfield information from the unsteady force fluctuations on the blade, Lowson's equation [4] is employed in this study. The purpose of this paper is to investigate the effects of rotating velocity, flow rate, cut-off distance and number of blades on the noise of a centrifugal fan. In order to compare to the experimental data, the centrifugal impeller with a wedge introduced by Weidemann [5] is used in the numerical calculation and the results are compared with the Weidemann's experimental data in the following sections.

*Corresponding author. Tel.: +82-2-818-7993; fax: +82-2-867-9629.
E-mail address: whjeon@lge.com (W.-H. Jeon).

0022-460X/03/$ - see front matter
doi:10.1016/S0022-460X(02)01582-1

2. Non-dimensional parameters

2.1. Flow coefficient and head coefficient

Flow coefficient is defined as

$$\phi = \frac{Q}{\pi b D_2 u_2}, \tag{1}$$

where Q and b mean the flow rate and width of the impeller, respectively; D_2 and u_2 mean the outer diameter of the impeller and the tip velocity of the impeller exit, respectively.

Head coefficient is defined as

$$\Psi = \frac{gH}{u_2^2}, \tag{2}$$

where H is the calculated head and g is the gravity acceleration.

2.2. Strouhal number

The most important non-dimensional variable for the aeroacoustics is the Strouhal number which is defined as

$$St = \frac{fD}{U}, \tag{3}$$

where D means the characteristic length of the object and U is the flow velocity. This non-dimensional variable is used to predict the frequency information of the flow noise. In the fan noise case the Strouhal number is modified as follows:

$$St = \frac{\pi}{Z}\frac{fD}{U} = \frac{f\hat{D}}{U}, \tag{4}$$

where Z is the number of impeller blades. In this definition, the characteristic length D is changed to $\hat{D}(= \pi D/Z)$. The Strouhal number is 1 for the BPF and 2 for the second harmonic frequency.

3. Numerical methods

In this paper, computations are focused on the amplitude of tonal noise from the centrifugal impeller. The discrete tone noise is generated due to the interaction between the cutoff in the casing and the rotating impeller. To simulate the noise generation mechanism, only an impeller and a wedge are considered without the casing, and the results are compared with experiment data as shown in Fig. 1.

It is assumed that the impeller rotates with a constant angular velocity and the flow field of the impeller is incompressible and inviscid. The flow fields are calculated by the DVM. The impeller has Z number of blades and each blade has nc number of elements. Bound vortices are located at the 1/4 point of each element and control points are taken at the 3/4 point of the element. Wake vortices are shed at the trailing edge of the impeller at every time step to satisfy the Kelvin's theorem. Shed vortices are convected with the local induced velocity. The inlet flow is modelled as

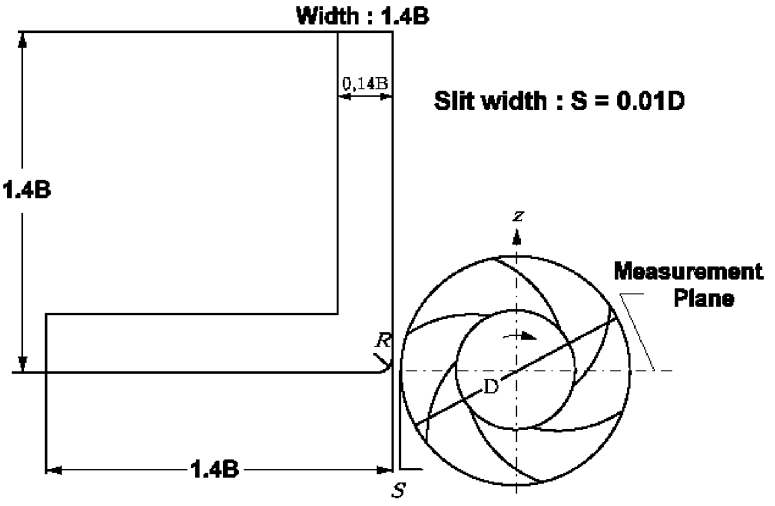

Fig. 1. Dimensions of the impeller and wedge [5].

a point source located at the center of the fan. The wedge is modelled as constant source panels where the control points are taken at the center of the element. The induced velocity at a point of the body ($\mathbf{x}_{cj}$) is calculated as

$$\mathbf{U}(\mathbf{x}_c, t) = \mathbf{U}_Q(\mathbf{x}_c, t) + \mathbf{U}_{bv}(\mathbf{x}_c, t) + \mathbf{U}_{wv}(\mathbf{x}_c, t) + \mathbf{U}_{sp}(\mathbf{x}_c, t). \tag{5}$$

The four terms on the right-hand side represents the velocity at $\mathbf{x}_{cj}$ induced by the point source, the velocity induced by bound vortices of the impeller, the velocity induced by wake vortices and the velocity induced by source panels, respectively. The shed vortices are convected with the local velocities.

The unknown strengths of the bound and wake vortices and the source panels are calculated with the normal boundary condition, that is there is no flow across the surface boundary (Eq. (6)) and Kelvin's theorem (Eq. (7a)) [1,6]:

$$[\mathbf{U}_Q(\mathbf{x}_c; t)_j + \mathbf{U}_{bv}(\mathbf{x}_c; t)_j + \mathbf{U}_{wv}(\mathbf{x}_c; t)_j + \mathbf{U}_{sp}(\mathbf{x}_c; t)_j] \cdot \mathbf{n}(\mathbf{x}_c)_j = \begin{cases} \Omega(\mathbf{n}(\mathbf{x}_c)_j \times \mathbf{x}_{cj}(t)), & \textit{impeller}, \\ 0, & \textit{wedge}, \end{cases} \tag{6}$$

$$\frac{D\Gamma_m(t)}{Dt} = 0, \tag{7a}$$

$$\left[\sum_{k=1}^{nc} \Gamma_{bk}(t) + \sum_{k=1}^{nv} \Gamma_{wk}(t)\right]_m = 0. \tag{7b}$$

Here, Γ_m is the total circulation of the mth blade, which includes the circulations of bound vortex (Γ_b) of the blade and shed wake vortex (Γ_w). And m, nc and nv mean the number of blades, and elements at each blade and shed vortex particles, respectively.

The force on each element of the blade is calculated by the unsteady Bernoulli equation:

$$\mathbf{F}_{nj} = \rho\left\{\mathbf{U}(\mathbf{x}_c)\cdot\boldsymbol{\tau}_j\frac{\Gamma_{bj}}{\Delta s_j} + \frac{\partial}{\partial t}\sum_{k=1}^{j}\Gamma_{bk}\right\}\Delta s_j, \tag{8}$$

where $\mathbf{F}$, $\boldsymbol{\tau}$ and Δs_j are the normal force on the element, the tangential vector of the element and the length of that element, respectively. ρ is the density of working fluid.

In 1965, Lowson derived the formula for the acoustic field generated by moving point force from the wave equation [4]. The equation was derived for one point force case, and we apply the equation to each element of the blade:

$$P - P_o = \left[\frac{x_i - y_i}{4\pi a_o r^2(1-M_r)^2}\left\{\frac{\partial F_i}{\partial t} + \frac{F_i}{1-M_r}\frac{\partial M_r}{\partial t}\right\}\right], \tag{9}$$

where

$$M_r = \frac{M_i r_i}{r}. \tag{10}$$

Eq. (9) indicates that the acoustic pressure by a moving point force is calculated using the time variation of force and acceleration. By applying this equation to each blade element, we can predict the acoustic pressure in a free field. The effects of the scattering and reflection due to the wedge are not considered; therefore, only the pattern of the noise source and its radiation to the free field can be estimated.

If one wishes to analyze the centrifugal fan with the volute casing, an additional procedure is necessary. The sound generated from the impeller will be scattered and reflected from the volute casing. Therefore, the analysis of the acoustic field of the volute casing with the aeroacoustic source is necessary for the complete prediction. This method was developed by Jeon and Lee and verified with experimental data [3]. However, the effects are small for the present case of the centrifugal impeller with a wedge.

4. Numerical results

The centrifugal impeller with a wedge placed close to the impeller tip is numerically analyzed. Weidemann used the same configuration of the impeller and a wedge for the study of acoustic similarity law [5]. The impeller has 6 blades and rotates at 1200–4100 r.p.m. The inlet diameter and inlet angle of the impeller are 0.112 m and 23.4°, and the outlet diameter and outlet angle are 0.28 m and 33.5°. Numerical calculations of the flow field are conducted up to 30 non-dimensional times, where one non-dimensional time means one revolution of the impeller. The impeller rotates 6° for each computational time step. Point for measurement and numerical calculation is located 1.96 m apart from the impeller center to the right-hand side of Fig. 1. Fig. 2 shows the variation of the strength of shed vortex at each blade in the case of 3000 r.p.m. The strength of each wake vortex varies periodically and this pattern is similar for each blade. These changes of the strength cause the periodic variation of the force at each blade element. Because of this unsteady rotating force of the impeller, discrete tones at BPF and its higher harmonics are generated. The distribution of shed vortex particles are shown in Fig. 3 for selected times. The circular symbol

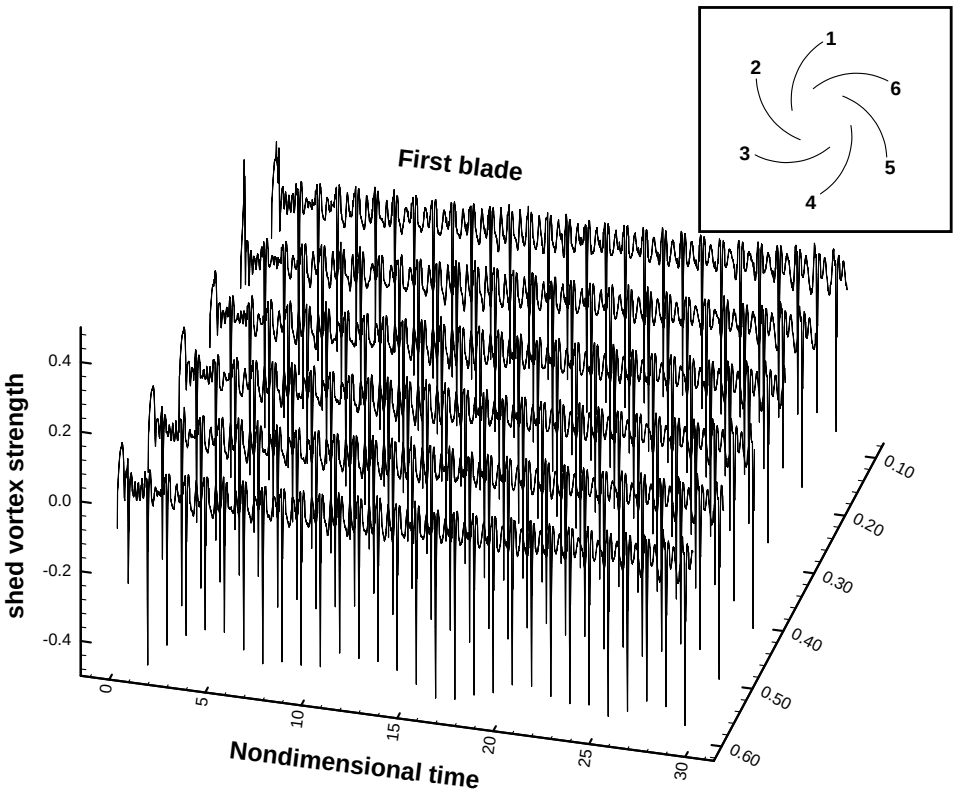

Fig. 2. Variations of the shed vortex strength with time at each blade.

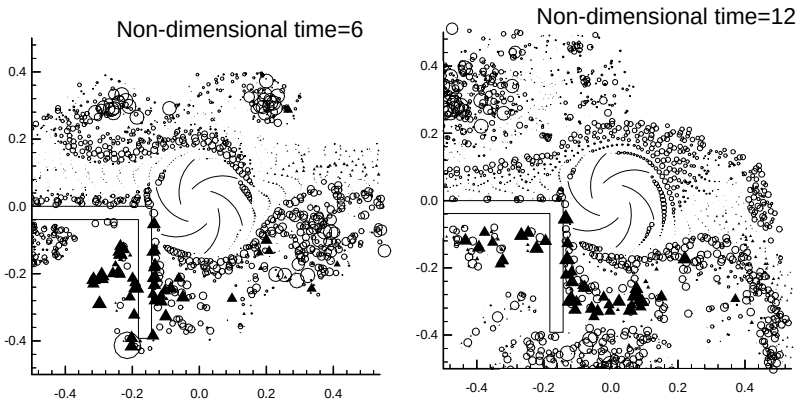

Fig. 3. Distributions of the shed vortex particle.

represents clockwise rotating vortex particle, and the triangular symbol represents counter-clockwise rotating vortex particle. The size of the symbol indicates the strength of the shed vorticity. Impeller rotates in the counter-clockwise direction. We can find that the direction of

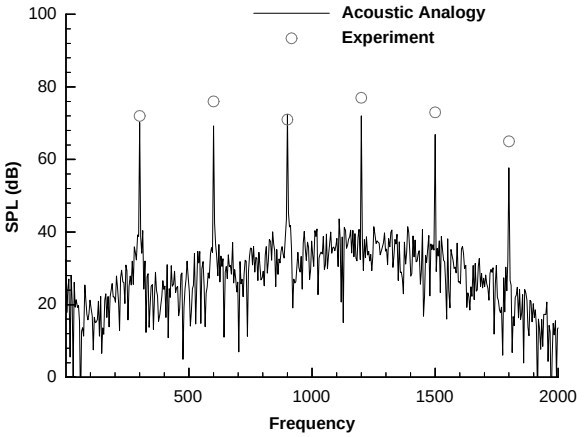

Fig. 4. Comparison of numerical and experimental acoustic spectra.

shed vortex is changed as the impeller passes the wedge. As the impeller comes close to the wedge, the higher negative vortices are generated at the tip of the blade. These variations occur periodically and the unsteady fluctuation of the head is due to this periodic interactions.

Predicted acoustic pressure data are shown in Fig. 4. In the spectrum, it is shown that not only the peak frequencies but also the amplitudes of the tonal sound are similar to the experimental data. Hollow circle symbols represent measured data [5], and solid line is the spectra of the acoustic pressure predicted by Lowson's equation. The amplitudes at the blade passage frequency and its harmonics are much higher than that of the broadband noise because of the small gap distance between the impeller tip and the wedge.

In this paper, numerical parameters, such as rotating speed, flow rate, cut-off distance and number of blades of the impeller, are changed to identify the acoustic characteristics of the centrifugal impeller.

First, the effect of the rotating speed is considered. The rotating speed is changed from 1200 to 4100 r.p.m. The overall sound pressure level (SPL) was calculated for various r.p.m.s. The peaks of the overall SPL at six peak frequencies are traced in Fig. 5. This pattern is similar to the Weidemann's results [5]. From the acoustic similarity law and the measured data by Weidemann, it is known that the acoustic pressure is proportional to $U^{2.8}$ [1,5] which is consistent with Weidemann's result as shown in Fig. 6.

Second, the effect of the cut-off distance on the acoustic pressure is calculated numerically. The cut-off distance (δ) is varied from 0.0028 m to 0.028 m. As the cut-off distance increases, the sound pressure level decreases as shown in Fig. 7. The amplitudes at higher harmonic frequencies decrease more steeply than those at BPF as the cut-off distance increases. In the case of 0.0028 m cut-off distance, the amplitudes at BPF and its higher harmonic frequencies peaks are similar. But for the 0.028 m cut-off distance case, the sound pressure level at BPF is 30 dB higher than that at the fourth harmonic frequency. In Fig. 8, the theoretical head with no loss term is shown for different cut-off distances. Fig. 8 shows the tendency of the head change for various rotating velocities.

Third, the effect of the number of blades on the sound pressure is numerically calculated. The number of blades is changed from 4 to 12. In this case, the impeller rotates 3° during each time

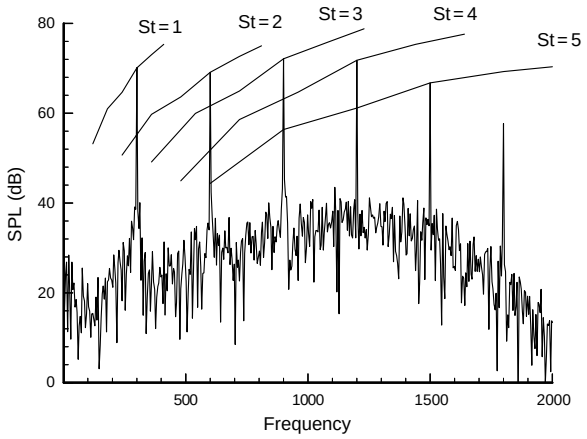

Fig. 5. Sound pressure level of peak frequency by changing rotating r.p.m.

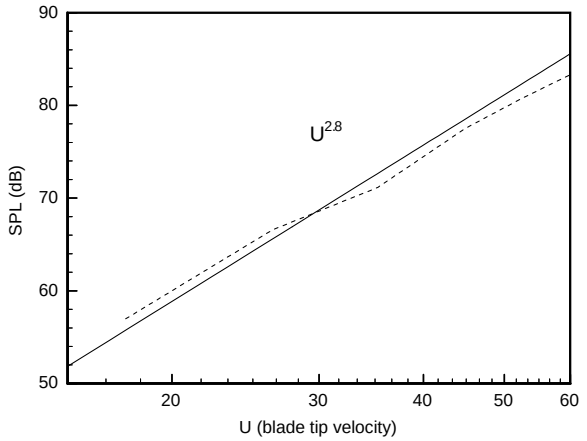

Fig. 6. Determination of the exponent of Mach number (dashed: calculated result).

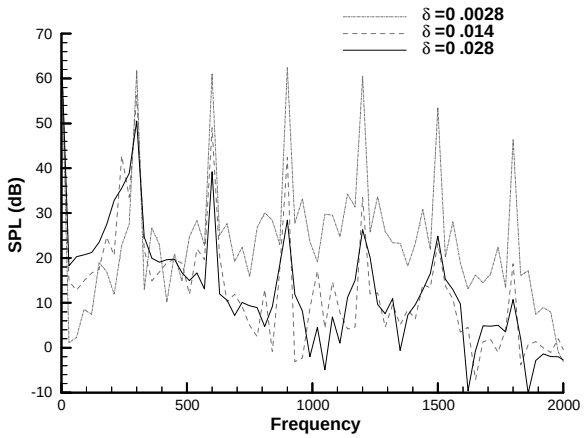

Fig. 7. Variations of spectrum with slit width change.

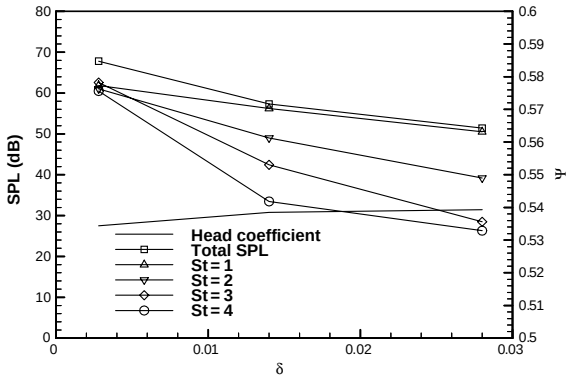

Fig. 8. Variations of SPL and head with slit width change.

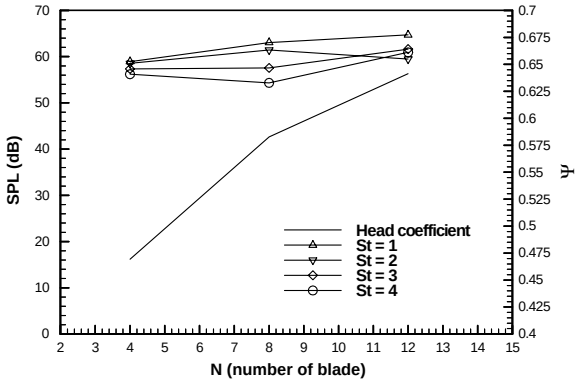

Fig. 9. Variations of SPL and head with blade number change.

step. In the numerical calculation, the number of blades does not effectively change the acoustic pressure comparing with the cut-off distance. As the number of blades increases, the sound pressure level at BPF increases slowly as shown in Fig. 9. However, the head increases rapidly. These results show that the noise reduction method proposed by DLR is appropriate, even though the method was applied in an axial fan [7]. They reduce the diameter of the fan and increase the number of blades. If the diameter of the impeller is reduced, then the performance and noise will be reduced. Therefore, in order to compensate the performance reduction, the number of blades should be increased. Finally, low-noise impeller can be made without the loss of performance [7].

Fig. 10 shows the results of the flow rate change. The variation of head shows the characteristics of the general performance curve of a centrifugal fan with the change of the flow rate coefficient from 0.112 to 0.14, but the level of the noise is almost constant. Eq. (11) shows the general fan sound law [8]. The general fan sound law shows that the change of the flow rate coefficient from 0.112 to 0.14 results in a change of noise by about 0.5 dB. This result is similar to the numerical one:

$$SPL = 10\log_{10} Q + 10\log_{10} P^2 + L_s, \tag{11}$$

where L_s is the specific noise level.

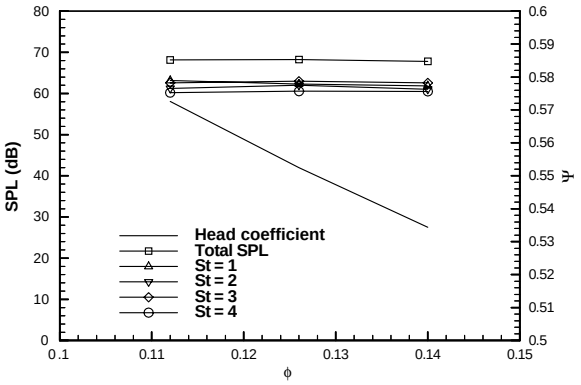

Fig. 10. Variations of SPL and head with flow rate change.

If the flow rate is reduced, the flow pattern is changed such that the flow is separated at the leading edge of the blade and the broadband noise increases. In this case, another new method should be employed in order to calculate the leading edge separation [8]. So, we restrict the change of the flow rate to a small range.

From the above numerical analyses, it is confirmed that the cut-off distance is the most important factor for the noise of a centrifugal fan. The SPL at higher harmonic frequencies decreases very steeply as the cut-off distance increases.

5. Conclusions

By using a numerical prediction method for the centrifugal fan noise, the characteristics of acoustic pressure from the centrifugal impeller and wedge system were studied. Numerical results and the measured data showed a consistency. The effects of design parameters, such as the rotating velocity, the cut-off distance and the number of blades of the impeller, on the noise of the fan were investigated. It was found that the most important factor for the noise of the centrifugal fan, is the cut-off distance. The cut-off distance changes the sound pressure levels not only at BPF but also at higher harmonics. As the cut-off distance increases, the amplitudes at higher harmonic frequencies decrease very steeply. It was also observed that the number of blades does not affect the noise level significantly.

References

[1] Wan-Ho Jeon, Duck-Joo Lee, An analysis of the flow and aerodynamic acoustic sources of a centrifugal impeller, Journal of Sound and Vibration 222 (3) (1999) 505–511.

[2] Wan-Ho Jeon, Duck-Joo Lee, An analysis of the flow and sound field of a centrifugal fan located near a wedge, Fifth AIAA/CEAS Aeroacoustics Conference, 99-1830, 1999.

[3] Wan-Ho Jeon, Duck-Joo Lee, An analysis of sound field of a centrifugal fan with volute casing, Sixth AIAA Aeroacoustics Conference, AIAA/CEAS 2000-2092, 2000.

[4] M.V. Lowson, The sound field for singularities in motion, Proceedings of the Royal Society in London, Series A 286 (1965) 559–572.
[5] J. Weidemann, Analysis of the relation between acoustic and aerodynamic parameters for a series of dimensionally similar centrifugal fan rotors, NASA TT F-13, 1971, p. 798.
[6] M. Kiya, A. Kusaka, Discrete vortex simulation of separated unsteady flow in a centrifugal impeller, Soviet Union–Japan Symposium on Computational Fluid Dynamics, September, 1988, pp. 1–7.
[7] H.H. Heller, DLR's involvement in European aviation noise research on fixed and rotary wing aircraft, Fifth AIAA/CEAS Aeroacoustics Conference Keynote Lecture, 1999.
[8] W. Neise, Review of fan noise generation mechanisms and control methods, An International INCE Symposium, 1992, pp. 45–56.